

Research Article

## Samarium Promoted Ni/Al<sub>2</sub>O<sub>3</sub> Catalysts for Syngas Production from Glycerol Pyrolysis

Mohd Nasir Nor Shahirah<sup>1</sup>, Bamidele V. Ayodele<sup>1</sup>, Jolius Gimburn<sup>1,2</sup>, Chin Kui Cheng<sup>1,2\*</sup>

<sup>1</sup>Faculty of Chemical Engineering & Natural Resources, <sup>2</sup>Centre of Excellence for Advanced Research in Fluid Flow (CARIFF), Universiti Malaysia Pahang, 26300 Gambang, Pahang, Malaysia

Received: 22<sup>nd</sup> January 2016; Revised: 1<sup>st</sup> February 2016; Accepted: 17<sup>th</sup> February 2016

### Abstract

The current paper reports on the kinetics of glycerol reforming over the alumina-supported Ni catalyst that was promoted with rare earth elements. The catalysts were synthesized via wet impregnation method with formulations of 3 wt% Sm-20 wt% Ni/77 wt% Al<sub>2</sub>O<sub>3</sub>. The characterizations of all the as-synthesized catalysts were carried out, viz. BET specific surface area measurements, thermogravimetry analysis for temperature-programmed calcination studies, FESEM for surface imaging, XRD to obtain diffraction patterns, XRF for elemental analysis, etc.. Reaction studies were performed in a stainless steel fixed bed reactor with reaction temperatures set at 973, 1023 and 1073 K employing weight hourly space velocity (WHSV) of 4.5×10<sup>4</sup> mL g<sup>-1</sup> h<sup>-1</sup>. Agilent GC with TCD capillary column was used to analyze gas compositions. Results gathered showed that the BET specific surface area was 2.09 m<sup>2</sup>.g<sup>-1</sup> for the unpromoted Ni catalyst while for the promoted catalysts, was 2.68 m<sup>2</sup>.g<sup>-1</sup>. Significantly, the BET results were supported by the FESEM images which showed promoted catalysts exhibit smaller particle size compared to the unpromoted catalyst. It can be deduced that the promoter can increase metal dispersion on alumina support, hence decreasing the size of particles. The TGA analysis consistently showed four peaks which represent water removal at temperature 373-463 K, followed by decomposition of nickel nitrate to produce nickel oxide. From reaction results for Sm promotion showed glycerol conversion, X<sub>G</sub> of 27% which was 7% higher than unpromoted catalyst. The syngas productions were produced from glycerol decomposition and created H<sub>2</sub>:CO product ratio which always lower than 2.0. The H<sub>2</sub>:CO product ratio of 3 wt% Sm promoted Ni/Al<sub>2</sub>O<sub>3</sub> catalyst was 1.70 at reaction temperature of 973 K and glycerol partial pressure of 18 kPa and suitable enough for Fischer-Tropsch synthesis. Copyright © 2016 BCREC GROUP. All rights reserved

**Keywords:** Glycerol; Pyrolysis; Ni/Alumina catalysts; Rare earth promoters; Kinetic reactions; Syngas

**How to Cite:** Shahirah, M.N.N., Ayodele, B.V., Gimburn, J., Cheng, C.K. (2016). Samarium Promoted Ni/Al<sub>2</sub>O<sub>3</sub> Catalysts for Syngas Production from Glycerol Pyrolysis. *Bulletin of Chemical Reaction Engineering & Catalysis*, xx (xx): xxx-xxx (doi:10.9767/bcrec.xx.xx.10050.xxx-xxx)

**Permalink/DOI:** <http://dx.doi.org/10.9767/bcrec.xx.xx.10050.xxx-xxx>

### 1. Introduction

For the last decades, glycerol (propane-1,2,3-triol) is an oxygenated organic compound

that has been used as an additive in the food, cosmetic, drugs and pharmaceutical industries [1]. The feasibility of glycerol to function as a reactant in some catalytic processes for the production of commodities has been evaluated in some of the past literature [1,2].

Glycerol has been proposed as a feedstock for several productions, such as: acrolein [3],

\* Corresponding Author.

E-mail: [chinkui@ump.edu.my](mailto:chinkui@ump.edu.my) (C.K. Cheng)

synthesis gas [4], hydrogen [5], and also as an additional transportation fuel via Fisher-Tropsch synthesis [6]. Theoretically, 4 moles of hydrogen and 3 moles of CO can be produced as gaseous product from 1 mole of glycerol. Gasification, pyrolysis or steam reforming could lead to a very satisfying performances [2].

Steam reforming of glycerol over ceria-supported Ir, Co, and Ni catalysts for production of hydrogen was studied [7]. The same case for the reforming of glycerol and its aqueous solution over nickel-based catalyst was determined [8]. For the gas phase pyrolysis of glycerol in steam produce in a laminar flow reactor successfully reported by Stein *et al.* [9]. Furthermore, from the pyrolysis of glycerol in N<sub>2</sub> in a packed bed tubular for production of syngas was performed by [10]. The thermal decomposition of glycerol in near-critical and supercritical water has been finalized by Buhler *et al.* [8]. Apart from that, the pyrolysis of the crude glycerol from biodiesel production plant was achieved by thermogravimetry coupled along with Fourier transform infrared spectroscopy in current work [2,11].

Significantly, this work aims to expand the study of production of syngas from glycerol pyrolysis over rare earth promoted Ni/Al<sub>2</sub>O<sub>3</sub> catalyst in a stainless steel fixed bed reactor. There are several novelties of the current work. Firstly, raw material (glycerol) was normally produced from biodiesel production as a by-product. But, the process is slow, expensive and produces low yield. In this case, the glycerol will act as a raw material undergoing reliable process to produce useful products such as syngas. The second aspect is the employed catalysts. Most of the time, common rare earth promoters like La and Ce were employed. Rare earth metal like Samarium is rarely studied, therefore was promoted into Ni/Al<sub>2</sub>O<sub>3</sub> catalyst in this study. The development of novel process is also involved. From previous study, catalytic reforming shows an impressive performance on syngas production [12,13]. The H<sub>2</sub>O or CO<sub>2</sub> was used together with raw material in the reforming process as gasifying agent. But, this work investigates a direct catalytic reaction of glycerol molecule itself. Ni catalysts supported on MgAl<sub>2</sub>O<sub>4</sub> promoted with rare earth have shown an impressive catalytic performance in ethanol steam reforming in other previous works [14]. Therefore, the primary objective of the current work is to study direct catalytic reaction of glycerol for syngas production over Ni/Al<sub>2</sub>O<sub>3</sub> catalyst promoted with rare earth metal, samarium.

## 2. Materials and Method

The alumina support was pretreated in a muffle furnace (Carbolite) at temperature of 1073 K for 6 h using a heating rate of 10 °C/min. Then, it was screened to 140-425 μm particle range. The freshly screened alumina was precisely weighed, then transferred into a beaker that contained desired amount of aqueous solution of Ni/(NO<sub>3</sub>)<sub>2</sub>.6H<sub>2</sub>O and Sm(NO<sub>3</sub>)<sub>3</sub>.6H<sub>2</sub>O in order to prepare 3wt%Sm-20wt%Ni/77wt%Al<sub>2</sub>O<sub>3</sub> catalyst. For the unpromoted 20wt% Ni/80wt%Al<sub>2</sub>O<sub>3</sub> catalyst, it was produced via the same method. To complete the impregnation procedure, the slurry was magnetic-stirred at 6.0 to 8.0 rpm (based on slurry condition) for 3 h at ambient condition, then oven-dried at 393 K for overnight. The dried catalysts were then air-calcined at 1073 K for 5 h. Finally, the calcined catalyst was crushed and sieved to 140-250 μm particle range for reaction studies.

For the x-ray diffraction (XRD) measurement, Shimadzu diffractometer model XRD-6000 employing Ni-filtered CuK<sub>α</sub> with a wavelength (λ) of 1.5418 Å at 40mA and 45 kV was used, with scanning ranged 10° to 80°. Based on the Scherrer equation [15], the crystalline size of the catalysts was calculated:

$$D_p = \frac{0.90 \times \lambda}{\beta \times \cos\theta} \quad (1)$$

where  $D_p$  is known as crystallite size,  $\lambda$  is the wavelength of the radiation,  $\beta$  is a half of the maximum intensity peak and  $\theta$  is the half of the diffraction angle. In order to determine the calcination profiles of the uncalcined dried catalysts and to ensure metal oxide formation by decomposition of metal nitrate, the TGA (Q5000-model) analysis was performed from room temperature to 873 K. The ramping rates operated were 10, 15 and 20 K/min under air purging consists of with 20 ml/min of O<sub>2</sub> and 80 ml/min of N<sub>2</sub>. BET analysis was employed to calculate the surface area of the catalysts. Moreover, liquid N<sub>2</sub> was used as adsorbate and 77 K was set as temperature. Density of the catalysts for N<sub>2</sub>-physisorption was obtained from the Gas pycnometer (1340 AccuPyc). Water was utilized as a blank with number of purge and cycles of 10. JEOL/JSM-7800F model of FESEM was applied for surface imaging of the catalysts. From 5kV of voltage acceleration with 10, 20 and 30 kx magnification, the image was detected.

Reaction glycerol pyrolysis was carried out in a stainless steel fixed bed reactor with 0.20 g of catalyst. The reaction temperatures were set at 973, 1023 and 1073 K. The total inlet flow rate was 150 ml.min<sup>-1</sup> culminating in weight hourly space velocity (WHSV) of 4.5×10<sup>4</sup> ml g<sup>-1</sup> h<sup>-1</sup>. In order to analyze the gas compositions, Agilent GC (Model no. 6890 series) with TCD capillary column was used. The GC has two packed columns, which are Supelco Molecular Sieve 13X (10 ft x 1/8 in OD x 2 mm ID, 60/80 mesh, Stainless Steel) and an Agilent Haysep DB (30 ft x 1/8 in OD x 2 mm ID, 100/120 mesh, Stainless Steel). The carrier gas used was He gas.

In addition the glycerol conversion to gaseous product (based on atom-H balance), yield of carbon and hydrogen were calculated based on Equations (2) to (4):

$$X = \frac{2 \times F_{H_2} + 4 \times F_{CH_4}}{8 \times F_{C_3H_8O_3, in}} \times 100 \quad (2)$$

$$Y_i = \frac{F_i}{3 \times F_{C_3H_8O_3, in}} \times 100 \text{ where } i = CO, CO_2 \text{ and } CH_4 \quad (3)$$

$$Y_{H_2} = \frac{2 \times F_{H_2}}{8 \times F_{C_3H_8O_3, in}} \times 100 \quad (4)$$

where I = CO, CO<sub>2</sub>, danCH<sub>4</sub> F<sub>i</sub> is the molar flow rate of component i.

### 3. Results and Discussion

#### 3.1 X-ray diffraction

Figure 1 shows the XRD pattern of both catalysts which indicates the existence of high crystallinity demonstrated by sharp peaks recorded at different 2θ. According to the graphs, during NiO at 37° in which impute its diffusion into the support to provide Ni-Al<sub>2</sub>O<sub>4</sub> at 36°, 38° and 63° [12,13].

Apart from that, the peaks indicates alike pattern for Sm promoted catalyst but has a

**Table 1.** Crystallite size for unpromoted Ni/Al<sub>2</sub>O<sub>3</sub> and 3 wt% Sm-Ni/Al<sub>2</sub>O<sub>3</sub> catalyst

Sample	Crystallite Size (nm)
20% Ni/Al <sub>2</sub> O <sub>3</sub>	39.22
3% Sm-20% Ni/77%Al <sub>2</sub> O <sub>3</sub>	42.12

lower intensity value in contrast to the unpromoted catalyst. Constant crystallite structure at the catalyst represent by the almost similar sharp peak pattern in NiAl<sub>2</sub>O<sub>4</sub> peak. The result was verified by FESEM image in which showed fine metal dispersion between the surfaces of the catalysts.

Table 1 summarizes the crystallite size for both sets of catalysts, with Sm promoted catalyst showing larger value compared to the unpromoted catalyst. The crystallite size was parallel with BET analysis that display higher surface area for Sm promoted Ni/Al<sub>2</sub>O<sub>3</sub> catalyst. The larger crystallite size could avoid pore blockage at the catalyst as well as increase the surface area.

#### 3.2. TGA analysis

By using air blanket to determine the weight loss associated with decomposition of nitrate, the thermal calcination profiles were obtained. Figure 2 illustrates the derivative weight changes profiles for both the unpromoted Ni/Al<sub>2</sub>O<sub>3</sub> and 3wt% Sm-Ni/Al<sub>2</sub>O<sub>3</sub> cata-

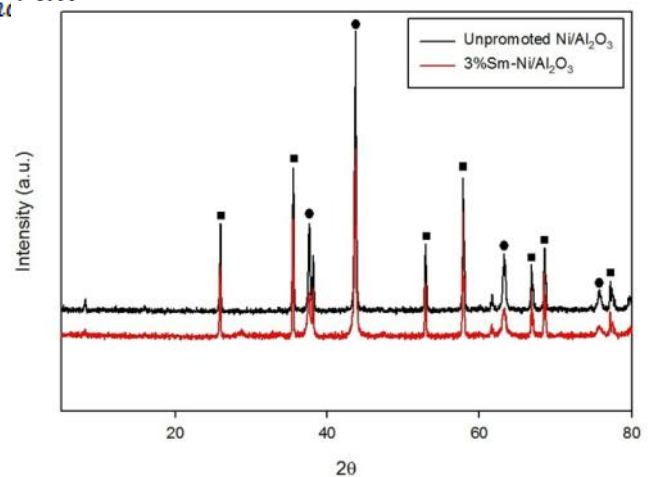


**Figure 1.** XRD pattern for calcined unpromoted Ni/Al<sub>2</sub>O<sub>3</sub> and 3 wt% Sm-Ni/Al<sub>2</sub>O<sub>3</sub> catalyst (■ Ni-Al<sub>2</sub>O<sub>4</sub>; ● NiO)

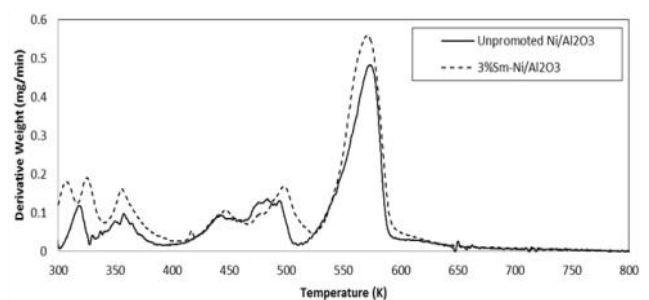


**Figure 2.** Derivative weight profiles of unpromoted Ni/Al<sub>2</sub>O<sub>3</sub> and 3 wt% Sm-Ni/Al<sub>2</sub>O<sub>3</sub>

lysts.

As shown in the Figure 2, it consistently recorded four peaks at temperature ranged 373 to 513 K that represent physical and hydration water removal. The sharp and large peaks recorded at temperatures from 513 to 643 K can be attributed to the decomposition of nickel nitrate and samarium nitrate to form NiO and Sm<sub>2</sub>O<sub>3</sub>, respectively. Beyond 643 K, the profile was flat. Therefore, the calcination of dried catalysts for actual reaction studies was carried out at temperature beyond 643 K to ensure complete removal of nitrate precursor.

### 3.3. BET specific surface area

As can be seen in Table 2, the BET specific surface area for Sm-promoted calcined catalyst was higher compared to the unpromoted; this observation was also verified by the subsequent

**Table 2.** Specific surface area for unpromoted Ni/Al<sub>2</sub>O<sub>3</sub> and 3 wt% Sm-Ni/Al<sub>2</sub>O<sub>3</sub> catalysts

Catalyst	BET Surface Area (m <sup>2</sup> g <sup>-1</sup> )
Unpromoted Ni/Al <sub>2</sub> O <sub>3</sub>	2.09
Sm promoted Ni/Al <sub>2</sub> O <sub>3</sub>	2.68

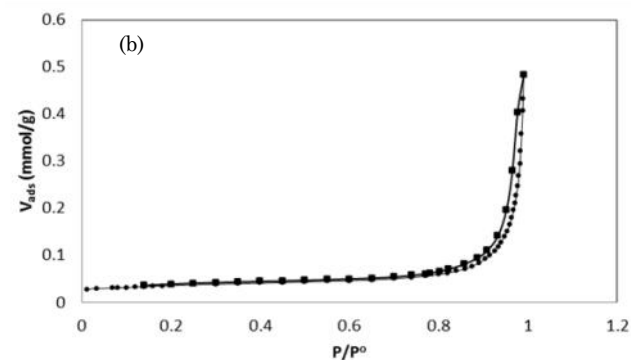
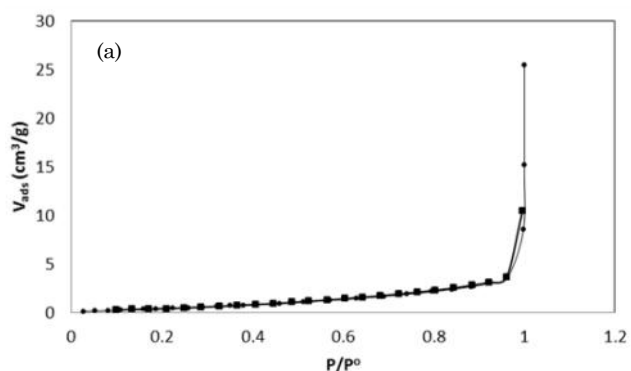


**Figure 3.** N<sub>2</sub> physisorption isotherms for calcined (a) unpromoted Ni/Al<sub>2</sub>O<sub>3</sub> and (b) 3 wt% Sm-Ni/Al<sub>2</sub>O<sub>3</sub> catalysts

FESEM analysis. The result was proven from low surface area for unpromoted catalyst in which effected from sintering from calcinations process earlier.

Based on N<sub>2</sub>-physisorption isotherms (cf. Figure 3), it is confirmed that the unpromoted Ni/Al<sub>2</sub>O<sub>3</sub> catalyst possessed mesoporous type V tunnel whilst upon 3 wt% Sm impregnation, the texture has changed to mesoporous type IV. The creation of new compositions by upgrade of the surface structure of the catalysts results in the change of interaction.

### 3.4. FESEM surface images

FESEM images showed the surface morphology of the catalysts as demonstrated in Figure 4. For Figure 4(a) labeled as unpromoted Ni/Al<sub>2</sub>O<sub>3</sub> catalysts the particle size as well as the porosity were contrast compared to with 3 wt% Sm-Ni/Al<sub>2</sub>O<sub>3</sub> (Figure 3(b)) catalysts. Due to the crystallite formation, the unpromoted catalyst present with the rougher and bulkier surface as well as larger particle size. Meanwhile for the Sm-promoted catalyst, the existence of metal such as Ni and Sm improved the surface structure due to the nature of the metals which avoid

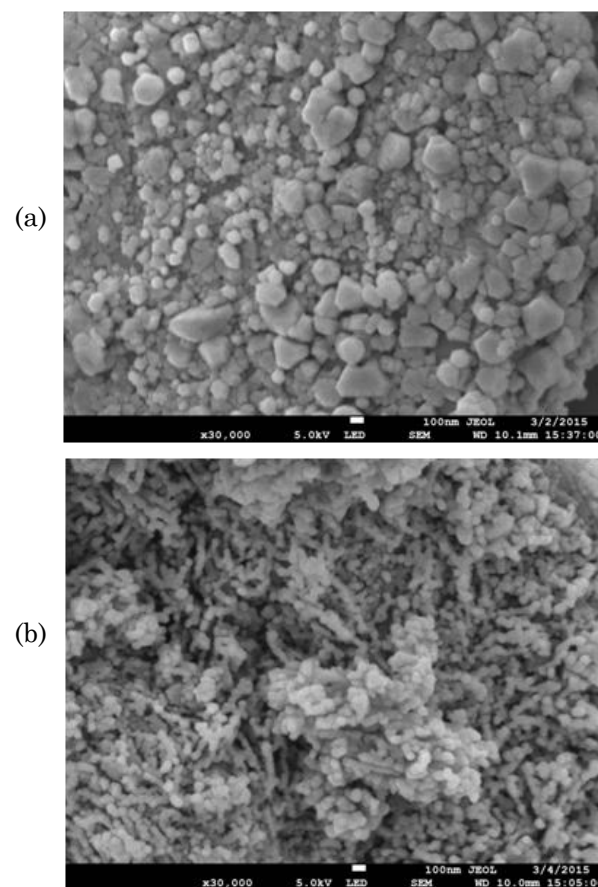


**Figure 4.** Catalysts structure for calcined (a) unpromoted Ni/Al<sub>2</sub>O<sub>3</sub> (b) 3 wt% Sm-Ni/Al<sub>2</sub>O<sub>3</sub>

the blockage of alumina pores. Hence, the presence of promoter catalyst can result in the increasing the surface area of calcined catalysts which was also supported by the BET results presented earlier.

From the images presented also indicated that the promoted catalyst has smaller particle size compared to the unpromoted catalyst. In order to avoid any formation of larger particles, the upgrade metal dispersion is necessary and to minimize sintering process, textural promoters play very important roles.

### 3.5. Catalytic reaction performance testing

The reaction studies that were included in the latest work are the effects of glycerol conversion and products yield. All the reactions part was run at ranging temperature 973 to 1073 K for 3 h with WHSV of  $4.5 \times 10^4$  ml  $g_{cat}^{-1} h^{-1}$  and 0.2 g of the catalysts.

In order to measure glycerol conversion,  $X_G$  and product yield,  $Y_i$ , partial pressure of glycerol,  $P_{gly}$  was varied along with various carrier gas (nitrogen) partial pressures,  $P_{N_2}$  at fixed temperature. Glycerol conversion profile indicates for unpromoted Ni/Al<sub>2</sub>O<sub>3</sub> and 3 wt% Sm-Ni/Al<sub>2</sub>O<sub>3</sub> catalysts over 3 h reaction time were

recorded in Figure 5.

According to the graph, glycerol conversion for Sm promoted Ni/Al<sub>2</sub>O<sub>3</sub> was higher than unpromoted Ni/Al<sub>2</sub>O<sub>3</sub> catalyst, additionally as securing steady state at early reaction. Therefore, glycerol composition was carried to production of syngas with assist by promoter of catalyst to upgrade reactant's internal diffusion into catalyst molecule. This situation related to FESEM images earlier which promoted catalyst could increase pores of the catalyst as well as improve reactant's internal dif-

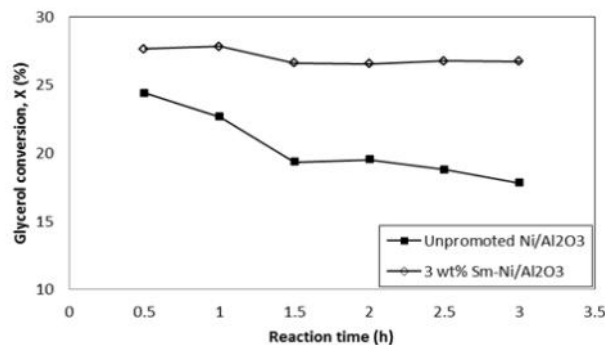


**Figure 5.** Glycerol conversion for unpromoted Ni/Al<sub>2</sub>O<sub>3</sub> and 3 wt% Sm-Ni/Al<sub>2</sub>O<sub>3</sub> at T = 973 K,  $P_{gly} = 14$  kPa and WHSV =  $4.5 \times 10^4$  ml  $g_{cat}^{-1} h^{-1}$  over 3 h reaction time

**Table 3.** H<sub>2</sub> yield over glycerol partial pressure for unpromoted Ni/Al<sub>2</sub>O<sub>3</sub>

Glycerol Partial Pressure (kPa)	Hydrogen Yield		
	973 K	1023 K	1073 K
4.5	22.64	24.00	18.97
9	27.51	19.76	26.01
13.5	17.91	18.00	21.66
18	17.71	18.56	16.29
22.5	12.52	21.74	20.70

**Table 4.** H<sub>2</sub> yield over glycerol partial pressure for 3 wt% Sm-Ni/Al<sub>2</sub>O<sub>3</sub> catalysts

Glycerol Partial Pressure (kPa)	Hydrogen Yield ( $Y_{H_2}$ )		
	973 K	1023 K	1073 K
4.5	22.33	22.53	25.74
9	20.59	23.11	25.97
13.5	24.49	23.79	25.79
18	20.33	22.47	20.05
22.5	20.44	21.11	27.43

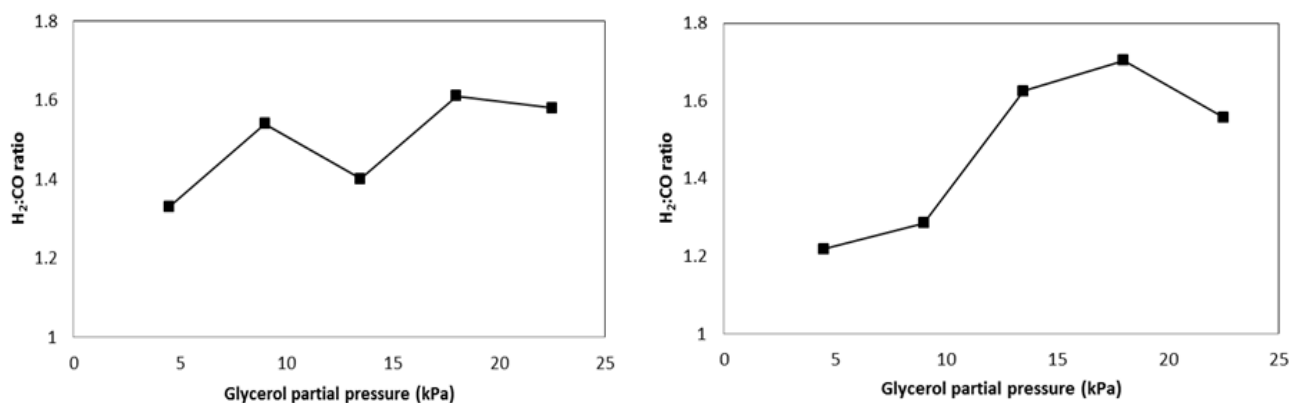


**Figure 6.** H<sub>2</sub>:CO product ratio versus glycerol partial pressure for a) unpromoted and b) 3 wt% Sm-Ni/Al<sub>2</sub>O<sub>3</sub> at T = 973 K and WHSV = 4.5×10<sup>4</sup> ml g<sub>cat</sub><sup>-1</sup>h<sup>-1</sup>

fusion.

The reactions were thoroughly explored by yield of hydrogen (H<sub>2</sub>) over glycerol partial pressure at various temperatures (973, 1023 and 1073 K) as shown in Tables 3 and 4. The yield of hydrogen indicated steady state reading at lower glycerol partial pressure which is at 4.5-13.5 kPa before reduce moderately at 18 kPa and showed increment pattern again at final partial pressure. The observation may result from the carbon laydown at the surface of catalysts. The observations also represent different stage of product yield by using varied temperature. According to H<sub>2</sub> yield, 1023 K temperature was pointed out as the most stable production in contrast to the other temperature. Hence, at temperature above 1023 K, carbon deposition may start to take place.

Furthermore, based on Figure 6 the H<sub>2</sub>:CO ratio can be observed. The value from the entire ratio recorded less than 2.0 at all operating temperatures. The highest H<sub>2</sub>:CO ratio recorded around 1.70 at glycerol partial pressure of 18 kPa. Therefore, all the ratio results feasible as the most appropriate alternatives for Fischer-Tropsch synthesis.

#### 4. Conclusions

The current work was presented the glycerol pyrolysis over 3 wt% Sm promoted Ni/Al<sub>2</sub>O<sub>3</sub> catalyst into syngas production which mainly produces H<sub>2</sub>. Sm promotion had larger BET surface area by doping 3 wt% Sm into a Ni/Al<sub>2</sub>O<sub>3</sub> catalyst based on physicochemical characterization of catalysts in which later verified and proved with FESEM surface images. Textural promoters take part in huge roles in order to minimize sintering and upgrade metal dispersion which were crucial to avoid formation of larger particles. The avail-









ability of promoter enhances the control the crystallite size to avoid pore blockage as provided by XRD results. Base on the reaction results for Sm promotion indicated glycerol conversion, X<sub>G</sub>, of 27% which was 7% higher than the unpromoted catalyst. From glycerol decomposition, the syngas productions were created and presented with H<sub>2</sub>:CO ratio which always lower than 2.0. The H<sub>2</sub>:CO ratio of 3 wt% Sm promoted Ni/Al<sub>2</sub>O<sub>3</sub> catalyst was 1.70 at reaction temperature of 973 K with recorded glycerol partial pressure of 18 kPa, suitable for Fischer-Tropsch synthesis.

#### Acknowledgements

This work is financially supported by RACE grant (RDU151302) of the Ministry of Education, Malaysia. Nor Shahirah Mohd Nasir is a grateful recipient of the MyBrain15 sponsorship by the same ministry.

#### References

- [1] Pagliaro, M., Ciriminna, R., Kimura, H., Rossi, M., Della Pina, C. (2007). From glycerol to value-added products. *Angew. Chem. Int. Ed.*, 46(24): 4434-.....
- [2] Hemings, E.B., Cavallotti, C., Cuoci, A., Faravelli, T., Ranzi, E. (2012). A Detailed Kinetic Study of Pyrolysis and Oxidation of Glycerol (Propane-1,2,3-triol). *Combustion Science and Technology*, 184(7-8): 1164–1178.
- [3] Chai, S.H., Wang, H.P., Liang, Y., Xu, B.Q. (2007). Sustainable production of acrolein: Investigation of solid acid–base catalysts for gas-phase dehydration of glycerol. *Green Chem.*, 9(10): 1130-.....
- [4] Simonetti, D.A., Kunkes, E.L., Dumesic, J.A. (2007). Gas-phase conversion of glycerol to synthesis gas over carbon-supported plati-

- num and platinum-rhenium catalysts. *J. Catal.*, **247**(2): 298-..... 
- [5] Cortright, R.D., Davda, R.R., Dumesic, J.A. (2002). Hydrogen from catalytic reforming of biomass derived hydrocarbons in liquid water. *Nature*, **418**(6901): 964-..... 
- [6] Valliyappan, T., Bakhshi, N.N., Dalai, A.K. (2008). Pyrolysis of glycerol for the production of hydrogen or syngas. *Bioresour. Biotechnol.*, **99**(10): 4476-..... 
- [7] Zhang, B., Tang, X., Li, Y., Xu, Y., Shen, W. (2007). Hydrogen production from steam reforming of ethanol and glycerol over ceria-supported metal catalysts. *Int. J. Hydrogen Energy*, **32**(13): 2367-..... 
- [8] Buhler, W., Dinjus, E., Ederer, H.J., Kruse, A., Mas, C. (2002). Ionic reactions and pyrolysis of glycerol as competing reaction pathways in near-and supercritical water. *J. Supercrit. Fluids*, **22**(1): 37-..... 
- [9] Stein, Y.S., Antal, M.J., Jones, M. (1983). A study of the gas-phase pyrolysis of glycerol. *J. Anal. Appl. Pyrolysis*, **4**(4): 283-..... 
- [10] Valliyappan, T., Ferdous, D., Bakhshi, N.N., Dalai, A.K. (2008). Production of hydrogen and syngas via steam gasification of glycerol in a fixed-bed reactor. *Top. Catal.* **49**(1): 59-..... 
- [11] Dou, B., Dupont, V., Williams, P.T., Chen, H., Ding, Y. (2009). Thermogravimetric kinetics of crude glycerol. *Bioresour. Technol.* **100**(9): 2613-..... 
- [12] Siew, K.W., Lee, H.C., Gimbun, J., Chin, S.Y., Khan, M.R., Taufiq-Yap, Y.H., Cheng, C.K. (2015). Syngas production from glycerol-dry (CO<sub>2</sub>) reforming over La-promoted Ni/Al<sub>2</sub>O<sub>3</sub> catalyst. *Renewable Energy* **74**(3): 441-447.
- [13] Cheng, C.K., Foo, S.Y., Adesina, A.A. (2011). Steam reforming of glycerol over Ni/Al<sub>2</sub>O<sub>3</sub> catalyst. *Catalysis Today*, **178**(1): 25-33.
- [14] Barroso, M.N., Gomez, M.F., Arrua, L.A., Abello, M.C. (2014). Co catalysts modified by rare earths (La, Ce or Pr) for hydrogen production from ethanol. *International Journal of Hydrogen Energy*, **39**: 8712-8719.
- [15] Siew, K.W., Lee, H.C., Gimbun, J., Chin, S.Y., Khan, M.R., Taufiq-Yap, Y.H., Cheng, C.K. (2015). CO<sub>2</sub> reforming of glycerol over La-Ni/Al<sub>2</sub>O<sub>3</sub> catalyst: A longevity evaluative study. *Journal of Energy Chemistry*, **24**(3): 3-10.

*Selected and Revised Papers from The International Conference on Fluids and Chemical Engineering (FluidsChE 2015) (<http://fluidsche.ump.edu.my/index.php/en/>) (Malaysia, 25-27 November 2015) after Peer-reviewed by Scientific Committee of FluidsChE 2015 and Reviewers of BCREC*